Vol 14 No 11, November 2005
1009-1963/2005/14(11)/2293-07

Chinese Physics

© 2005 Chin. Phys. Soc.
and IOP Publishing Ltd

Rectifying barrier at GaN/SiC hetero-junction studied with positron annihilation spectroscopy

Hu Yi-Fan(胡一帆)[a] and Beling C D[b]

[a] *Department of Physics, Huazhong University of Science and Technology, Wuhan 430074, China*

[b] *Department of Physics, University of Hong Kong, Hong Kong, China*

(Received 14 December 2004; revised manuscript received 23 March 2005)

Positron annihilation spectroscopy on GaN films grown on SiC substrate with MBE are presented. It is shown that the GaN/SiC interface is rectifying towards positrons, such that positrons can only travel from SiC to GaN and not vice versa. Potential steps seen by the positron at the GaN/SiC interface are calculated from experimental values of electron and positron work function. This "rectifying" effect has been successfully mimicked by inserting a thin region of very high electric field in the Variable Energy Positron Fit (VEPF) analysis. The built-in electric field is attributed to different positron affinities, dislocation and/or interface defects at the GaN/SiC interface.

Keywords: GaN, SiC, hetero-junction, positron, rectifying barrier
PACC: 6800, 7870B

1. Introduction

Wide band gap semiconductors, such as GaN and SiC, exhibit many attractive properties: the unique combination of the wide band gap, the high breakdown field (over 2 MV/cm), the high saturation velocity, good transport properties which make them ideal candidates for high-power, and high-frequency applications.[1−6] Rapid progress in the performance of microwave power transistors has been obtained, owing to the use of SiC substrates instead of sapphire, and take advantage of the high thermal conductivity and stability of SiC. Therefore, numerous studies have been devoted to improve the growth and microstructure of epitaxially grown GaN on SiC substrates. The main factors governing the transport properties are the band offsets at the interface. At present, some theoretical works are reported for this heterojunction system,[7−10] but there are few experimental data and large uncertainties still exist on the band offsets at the GaN/SiC heterojunction. It was not until 1997 that positron studies of GaN were performed by Dannefear *et al*[11] and Saarinen *et al.*[12] Since that time, beam-based positron Doppler broadening annihilation spectroscopy (PDBAS) has been demonstrated to be powerful in determining the defects structures at semiconductor interfaces. On the other hand, to produce a highly mono-energetic positron beam with high efficiency, some new moderator materials are expected. Recently, efficient re-emission from semiconductor materials for the moderators, such as diamond,[13] SiC,[14−16] GaN[16,17] have been found. A moderator constructed by using these materials can moderate positrons of several keV. Since the penetration depth of several keV positrons is a few hundred nanometres, one can make a semiconductor moderator with a depletion layer of several hundred nanometres in thickness by using a built-in potential of p-n junction. Some experiments have been done on these semiconductor moderators. The experimental results show that the re-emitted positron fraction from these moderators is quite high, and the field-assisting effect has been seen very easily.[18] In this work, we study by using variable energy positron annihilation spectroscopy (VEPAS), a variety of GaN epilayers grown on SiC substrates for different growth conditions. The plots of the line-shape parameter against the positron energy have been obtained. In the plots a peak in the S-parameter has been seen which is related to the GaN/substrate hetero-junction. This anomaly has been attributed to the fact that there is a rectifying potential step which prevents diffusing positrons in the GaN from entering the SiC substrate. The relative potential step of the energy levels of delocalized

positrons between the GaN and SiC is determined by the positron affinities of the materials.

2. Sample preparation

The MBE growth of GaN was carried out by using MBE growth system in the Department of Physics, University of Hong Kong. The deposition rate was 0.026nm/s and substrate temperature was 650°C. These conditions ensured a step flow growth mode as indicated by the absence of isolated islands observable by scanning tunnelling microscopy (STM). Sample heating was achieved by applying a DC current through the sample along the long side of the rectangular substrate (10×4 mm^2 in size). The voltage drop was 8 V and the current was 0.9A. For GaN growth, the Ga and N source fluxes were provided respectively from a conventional Knudson cell at the cell temperature 980°C and from a radio-frequency (RF) plasma generator (Oxford Applied Research, CARS25). The N_2 flow rate was 0.13 sccm (standard cubic centimetre per minute) and the RF power was 500W. The corresponding GaN/N flux ratio was measured to be approximately 2. To quench the growing surface, the DC heating power of the sample was simply switched off. At the same time, the source fluxes were stopped by closing the source shutters as well as by shutting down the RF power of the plasma unit. Two samples were constructed. The thickness of the first sample (M056) was 300nm, while the thickness of the second (M057) was 90nm. These thicknesses were checked by a step thickness profiler. Both samples were n type ($\sim10^{16}$cm^{-3}) but were not intentionally doped. The film crystal structure was wurtzite. The substrates for M056 and M057 were n-type ($\sim10^{18}$–10^{19}cm^{-3}) nominally flat 6H-SiC (0001 oriented) and vicinal 4H-SiC (0001 oriented) respectively. The vicinal angle for the latter sample was 3.5° and oriented towards the $(\bar{1}010)$ direction. GaN deposition was on the Si-face in both cases.

3. Experiments

Measurements on the GaN/SiC samples were made using the slow positron beam. The beam energy was varied from 30eV–35keV manually, with most data being taken in the 0–10keV range so as to cover the detail of the film and interface. The 511-keV annihilation radiation gamma photons were detected by using a high-purity Ge detector of 1.12keV resolution (FWHM). The detector energy signal was amplified by a single spectroscopy amplifier and digitized by a 16k channel multi-channel analyser. For each positron beam energy, a total of 7×10^5 counts were collected.

Doppler broadening of annihilation radiation spectroscopy (DBARS) has been used to measure the longitudinal component of the photon pair momentum, which in turn is the longitudinal component of the electronic momentum.

4. Experimental results

The energy spectrum measured $C(E)$ is the spectrum convoluted with the resolution function $R(E\gamma, E)$ of the system. We prefer to avoid deconvolution through a simpler device to deal with the DBARS spectrum. In this method, we analysed the spectrum by a ratio S or the "shape" parameter. This parameter, originally suggested by MacKenzie *et al* [19] is defined as

$$S = \frac{\int_{-a}^{a} C(E)\mathrm{d}E}{\int_{-\infty}^{\infty} C(E)\mathrm{d}E}, \qquad (1)$$

where $C(E)$ is the energy spectrum. The S-parameter is defined as the ratio between the areas of the central region to the whole area of the broadened 511keV peak. Positrons get trapped at neutral and negative vacancy defects because the missing positive ion core charge causes the particle to experience a potential well. The reduced valence and core electron density at a vacancy increase the lifetime of the trapped positron, and narrow the positron momentum distribution, since the relative proportion of valence to core annihilations increases. Thus decrease of the possibility of annihilation between decreasing positrons and core electrons leads to the increase of S-parameter.

The $S-E$ plots of the sample M056 and M057 were given in Fig.1(a) and Fig.1(b) respectively. It was found that a three-layer model comprising the

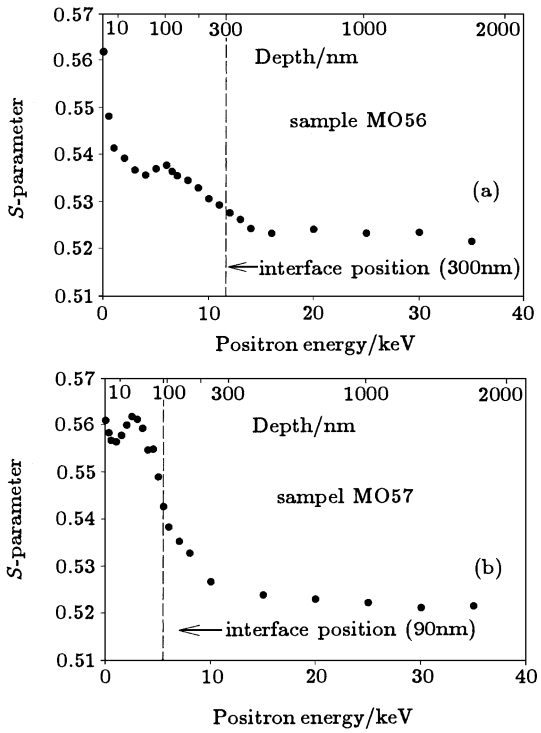


Fig.1. S parameter versus positron implantation energy for the thin GaN films with different thickness. (a)Sample MO56 with 300nm GaN/4H-SiC. (b) Sample MO57 with 90nm GaN/6H-SiC.

GaN film, the interface layer and the SiC bulk was the minimum model required to interpret these curves. The S-parameter for a given beam energy was thus given by

$$S(E) = F_{\rm s}(E)S_{\rm s} + F_{\rm GaN}(E)S_{\rm GaN} + F_{\rm I}(E)S_{\rm I} + (1 - F_{\rm s}(E) - F_{\rm GaN}(E) - F_{\rm I}(E))S_{\rm SiC}, \quad (2)$$

where $F_{\rm s}(E)$, $F_{\rm GaN}(E)$, and $F_{\rm I}(E)$ are the fractions of positrons annihilating in the surface, the GaN layer, and the interfacial region respectively. The surface fraction $F_{\rm s}(E)$ is characterized by the GaN's effective positron diffusion length $L^{\rm eff}_{\rm GaN}$. At low implantation energies, the S-parameter is high because it is more characteristic of the positron surface state. As the positron incident energy increases, the S-parameter drops because fewer positrons are able to diffuse back to the surface. It seems reasonable that $S_{\rm s}$ is higher than $S_{\rm GaN}$, because positrons at the surface experience less compression into interfacial regions, so that less high-momentum-core annihilations take place, and moreover para-positronium can form at the GaN surface.[20] It is very clear that both curves contain a peaked structure. In sample M056, the peak maximizes at ~6keV of incident positron energy which corresponds to 120nm depth. For the M057 sample the peak maximizes at ~3keV which corresponds to 24nm depth. Both these depths are those obtained by using the mean implantation depth formula

$$\overline{x} = 40E^{1.6}/\rho({\rm nm}). \quad (3)$$

The reason that such peaks occur can only be attributed to the contribution of the interfacial region, where, as a result of lattice mismatch there are large open volume sites which produce a high $S-$parameter. With this interpretation, however, one notices a striking disagreement between the interface depth as determined on the one hand by variable energy positron annihilation spectroscopy (VEPAS) and as, on the other hand, determined from the growth rate and step profiling measurement. For M056 the former depth is ~120nm while the later is 300nm. For M057 the former depth is ~24nm while the later is 90 nm. Moreover, the discrepancy is not removed performing VEPF fits to the data since the interface depths so obtained are almost identical to those obtained by using Eq.(3). This discrepancy is a real effect, and is shown as below.

5. Analysis and discussion

The S-parameter plots are analysed by using a software: VEPF.[21] A major question has been raised in the preliminary analysis above as to why it is that the depth of the interface as determined by the VEPF is clearly in error (see Fig.1). Binggeli and Ferrara examined the influence on the electronic valence-band-offset induced by a transformation from zinc-blende to wurtzite crystal structures in GaN/SiC.[9] Particularly, they investigated the band-offset dependence on the interface orientation, strain, heterovalency, and polytype. They found that local atomic interfacial relaxation has a major influence on the offsets of the heterovalent nitride interfaces. For the positrons, it is a little more complicated than for electrons. To facilitate discussion it is helpful to understand the quantities known as the positron affinity of GaN and SiC.

The relative position of the energy levels of delocalized positrons between different materials in contact are determined by one parameter, that is the positron affinity A_+ which can be used to estimate the positron diffusion constant.[22] The positron affinity was defined as the sum of the internal electron

and positron chemical potentials and has a negative value:[23]

$$A_+ = \mu_- + \mu_+. \tag{4}$$

It follows that the positron affinity is related with the electron work function ϕ_- and the positron work function ϕ_+ which are defined with respect to the vacuum level:

$$A_+ = -(\phi_- + \phi_+). \tag{5}$$

The measurement of ϕ_- and ϕ_+ thus allows an experimental method of finding A_+. Alternatively A_+ may be found from theory but with less reliability. Quote after the density-functional theory in local-density approximation[24] is used to calculate A_+. Alternatively the linear-muffin-tin orbital method within the atomic-spheres approximation[25,26] may be used. In the latter method the potentials and energy levels are given with respect to the so-called crystal zero level, which is defined as the zero of the Coulomb potential due to the nuclei and the electron density of the infinite solid.

For understanding how to derive Eq.(5) let us consider Fig.2. This diagram shows the electron and positron potentials and energy levels near a solid surface. It is shown that there are three very important

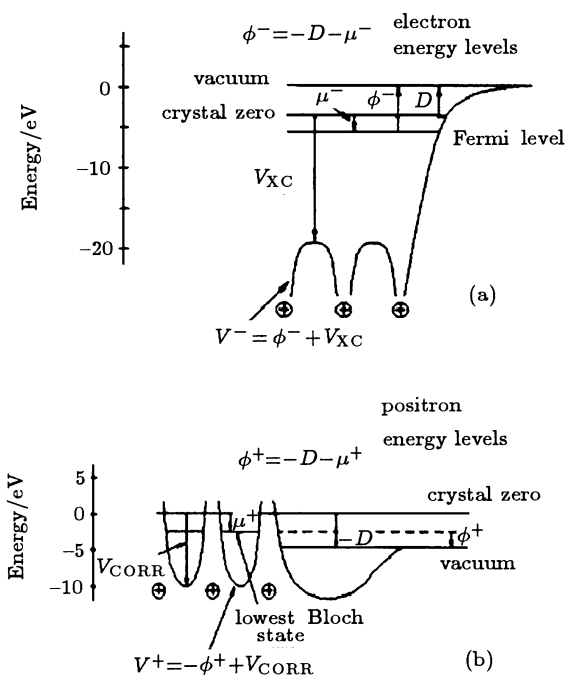


Fig.2. Electron (a) and positron (b) potentials and energy levels near a surface.

physics quantities: the surface dipole energy D, the electron chemical potentials, μ_- and μ_+, and the work functions ϕ_- and ϕ_+. The surface dipole energy D, is the change of the potential energy across the surface dipole. The electron chemical potential, μ_-, is the energy required to extract an electron from the Fermi level to the crystal zero. For the positron, the chemical potential, μ_+, is the energy required to extract the positron from lowest Bloch state to the crystal zero. For both electrons and positrons the work function, ϕ, is the energy required to extract the respective particle from the Fermi level to the vacuum. For electron, the relation among the three quantities is

$$\phi_- = D - \mu_-, \tag{6}$$

while, for positrons,

$$\phi_+ = -D - \mu_+, \tag{7}$$

where μ_+ and μ_- should be negative. Addition of Eqs.(6) and (7) and the definition of A_+ (Eq.4) leads to Eq.(5). It should be noted that in some materials such as GaN, SiC, GaAs *et al* the absolute value of D is larger than the absolute value of μ_+, which makes the work function for the positron negative – a feature that is of fundamental importance as regards the production of positron moderator for beams.

Figure 3 shows the electron and positron potentials and energy levels near a junction of two materials. The vertical scale corresponds to the particle energies

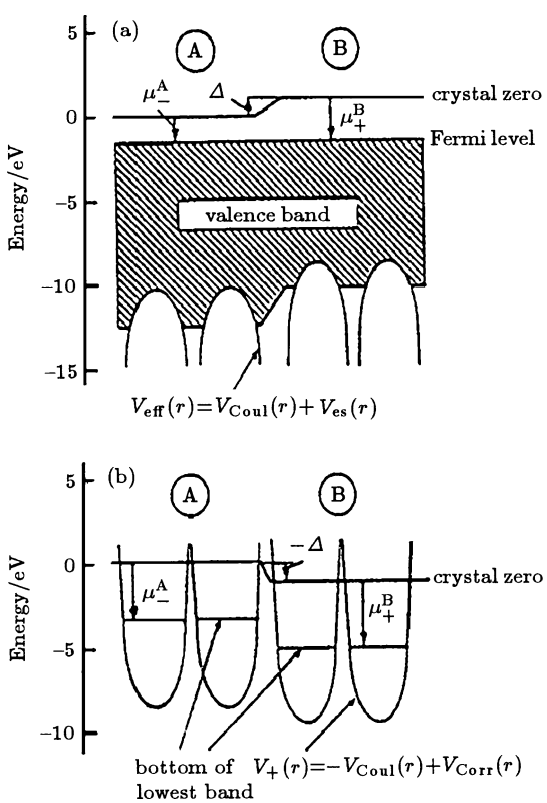


Fig.3. Electron (a) and positron (b) potentials and energy levels near a junction of two materials.

found at the junction between material A and B. On the electron diagram (a) Fermi levels equalize themselves via the formation of an interface dipole with the potential difference $\Delta = \mu_-^{\rm A} - \mu_-^{\rm B}$. For the positrons, the difference between the bottoms of the lowest band on the different sides of the interface is given by

$$\begin{aligned}\Delta E_+^{\rm A,B} =& E_+^{\rm A} - E_+^{\rm B} = \mu_+^{\rm A} - \mu_+^{\rm B} + \Delta \\ =& \mu_+^{\rm A} - \mu_+^{\rm B} + \mu_-^{\rm A} - \mu_-^{\rm B},\end{aligned} \tag{8}$$

which from the definition of A_+ becomes:

$$\Delta E_+^{\rm A,B} = A_+^{\rm A} - A_+^{\rm B}. \tag{9}$$

In application of Eq.(9), it should be noted that for a semiconductor the electron work function is rarely measured or reported. Instead the electron affinity χ_- is normally quoted, which is the energy required to remove an electron from the conduction band into vacuum. Thus one has for a semiconductor

$$A_+ = \mu_- + \mu_+ = -(\phi_- + \phi_+) = -(\chi_- + E_{\rm g} + \phi_+), \tag{10}$$

where $E_{\rm g}$ is the band gap. Table 1 gives some quantities required for the computation of A_+ for GaN and SiC.

Table 1. Some quantities required for the computation of A_+ for GaN and SiC.

	Electron band gap $E_{\rm g}$/eV	Electron affinity A_-/eV	Positron work function ϕ_+/eV	Positron affinity A_+/eV
GaN	3.4	4.06[27]	–2.4±0.3[28]	–5.06±0.3[27,28]
SiC	3.0	3.8[29]	–3.29±0.5[30]	–3.51±0.8[29,30]

One notes positron affinities of –5.06±0.3 eV and –3.51±0.8eV for GaN and SiC respectively. Therefore, the affinity difference across the hetero-junction of GaN/SiC is given by

$$\begin{aligned}\Delta E_+ =& A_+^{\rm GaN} - A_+^{\rm SiC} \\ =& -5.06 + 3.51 = -1.55 \pm 1.0{\rm eV}.\end{aligned} \tag{11}$$

This result suggests that a diffusing positron approaching the GaN/SiC interface will see a potential step of $\sim$ 1eV which will prevent it entering into the SiC. The reverse is true for the diffusing positron in the SiC approaching the interface that will just "fall" into the GaN. In order to mimic this "rectifying" behaviour with the VEPF software a strong electric field of $6\times10^5{\rm V\cdot cm^{-1}}$ was introduced into the $\sim$25 nm wide interface region. The effect of the rectifying potential hill on the VEPF analysis will be considered. The parameter values (α, m and n) used for the standard Markovian form of implantation profile $P(E,x)$ are given in Table 2 along with densities and sample thickness.

Table 2. S-parameters used in VEPF analysis of MBE grown GaN/SiC samples.

Materials	GaN	SiC
Density ρ	$6.1{\rm g\cdot cm^{-3}}$	$3.2{\rm g\cdot cm^{-3}}$
Implantation α	$36{\rm nm\cdot g\cdot cm^{-3}}$	$36{\rm nm\cdot g\cdot cm^{-3}}$
Parameter m	2.0	2.0
Parameter n	1.6	1.6
Thickness Δ of sample MO56	300nm	0.5mm
Thickness Δ of sample MO57	90nm	0.5mm

The resulting fits to the data are shown by the curves in Figs.4 and 5 in which a three-layer-model was assumed (layer 1= GaN layer, layer 2= interface layer and layer 3= SiC bulk). The diffusion length of SiC substrate is fixed to 69nm as obtained from $S(E)$ scanning a pure SiC on the reverse side of the sample. All other linear and non-linear parameters are fitted such as $S_{\rm s}$, $S_{\rm GaN}$, $S_{\rm I}$, $S_{\rm SiC}$, $S_{\rm epi}$, layer boundaries B_1 and B_2, and diffusion lengths $L_{\rm GaN}$.

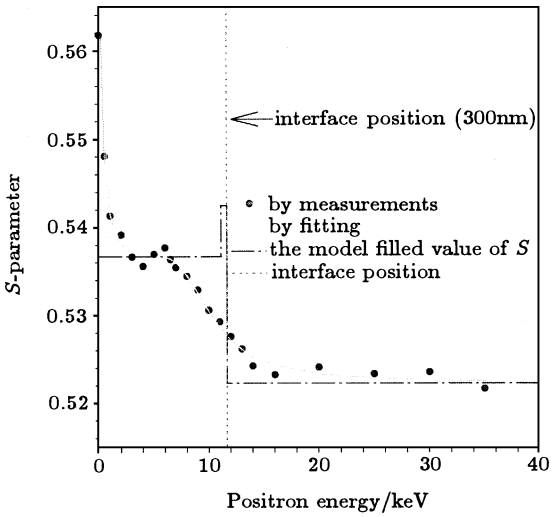


Fig.4. The VEPF fitting result for the Sample MO56.

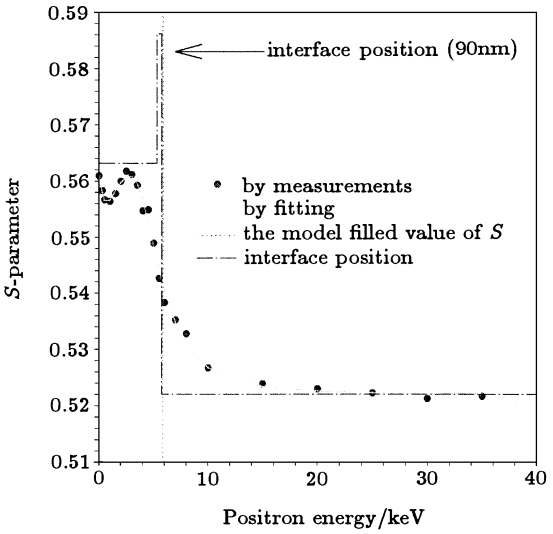


Fig.5. The VEPF fitting result for Sample MO57.

Table 3. VEPF fitting results.

Sample	S_s/nm	S_{GaN}/nm	S_I/nm	S_{SiC}/nm	B_1	B_2	L_{GaN}	L_{SiC}
MO56	0.5402(1)	0.5364(3)	0.6143(6)	0.5225(4)	278	299	12	69
MO57	0.5513(2)	0.5633(8)	0.5830(2)	0.5219(1)	82	100	12	69

Table 3 gives the VEPF fitting results. Under the effect of the potential step, some positrons are "reflected" back to the GaN layer or surface. Which makes the F_{GaN} and F_s becoming larger and finally makes the $S(E)$ becoming larger. As may be seen a very small diffusion length is required for the interface region in order to describe the data. It means that there is a strong built-in electric field in this region, and it is not surprising as this layer has large open volume defects, which trap positrons efficiently. In carrying out a study such as the present one, it may be hoped that information on the interface and film S-parameters could be gained through which the quality of these regions could be assessed. Table 3 shows that in the present study this is not possible, because of the strong inter-correlation that exists between S_{GaN} and S_I. Figure 6 gives the pictures of the potential steps seen by the positron at the GaN/SiC interface which are calculated from experimental values of electron and positron work function, and the three layer model area in VEPF analysis to represent the graded interface.

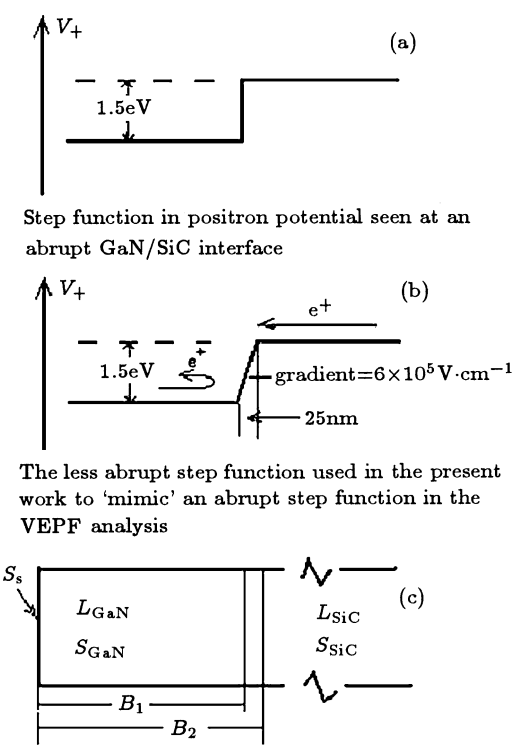


Fig.6. Potential steps seen by the positron at the GaN/SiC interface as calculated from experimental values of electron and positron work function. (a) The ideal abrupt junction, (b) The more realistic graded junction used in the present work and (c) The three layer model area in VEPF analysis to represent the graded interface.

6. Conclusion

A variety of MBE grown GaN epilayers on SiC substrates which were grown by using different growth conditions has been studied by using VEPAS. The plots of the line-shape parameter against the positron energy have been obtained. In the plots a peak in the S-parameter has been seen which is related to the GaN/substrate hetero-junction. The position of the peak has been found to be much closer to the sample surface than expected from simple mean implantation depth arguments. VEPAS data taken on two MBE grown GaN with SiC substrates have been analysed by using the VEPF software. It has also been found that if positrons are taken as freely moving across the GaN/SiC interface in both directions, results are obtained that cannot be made to agree with the known thicknesses of the GaN films. If, on the other hand, the potential step seen by positrons at the interface is catered for in VEPF analysis then the discrepancy is fully removed. This study shows the importance of knowing positron affinities when analysing VEPAS data. In general it is highly unlikely that positrons will have the same affinity to materials on both sides of an interface. The expected situation, then, will always be for "positron rectification"—inwards to the substrate outwards towards the film and surface—according to the sign of the potential step. The relative potential step of the energy levels of delocalized positrons between the GaN and SiC is determined by the positron affinities of the materials. Available data shows that positrons are expected to pass from the SiC to the GaN, but not vice-versa. This "rectifying" effect has been successfully mimicked by inserting a thin region of very high electric field in the VEPF analysis, and this built-in electric field can assist positron re-emission. Therefore, if a right film thickness is chosen, the hetero-junction as GaN/SiC should have the same function as a p-n junction in a semiconductor field assisted moderators constructed by using SiC or GaN. In future studies of these materials it will be necessary to choose a right thickness of GaN film and investigate the re-emitted positron fraction. If the built-in assist-electric-effect could be seen, one can make the best moderator for high efficiency moderation from these materials.

Acknowledgement

The authors would like to thank Shen Y Y, Fung S, Xie M H, Cheung S H, Brauer G and Anwand W for their continuing collaboration.

References

[1] Ponce F A, Krusor B, Major J S *et al* 1995 *Appl. Phys. Lett.* **67** 410
[2] Sood A K, Egerton E J, Puri Y R *et al* 2004 *Free Space Laser Communications* **IV:** 130
[3] Edmond J, Abare A, Bergman M *et al* 2004 *J. Crystal Growth* **272** 242
[4] Song B, Ling L and Cao P L 2004 *Chin. Phys.* **13** 489
[5] Feng D H, Jia T Q and Xu Z Z 2003 *Chin. Phys.* **12** 1016
[6] Zhou J J, Jiang R L, Sha J, Liu J, Shen B, Zhang R and Zheng Y D 2003 *Chin. Phys.* **12** 785
[7] Schaff W J, Wu H, Praharaj C J *et al* 2000 *Solid-State Electronics* **44** 259
[8] Rizzi A, Lantier R, Monti F *et al* 1999 *J. Vacuum Sci. & Tech.* B **17** 1674
[9] Binggeli N and Ferrara P 2001 *Phys. Rev.* B **63** 245306
[10] Majewski J A, Stadele M and Vogl P 1997 *III-V Nitrides; Materials Research Society Symp. Proc.* **449** 917
[11] Dannefaer D, Puff W and Kerr D 1997 *Phys. Rev.* B **55** 2182
[12] Saarinen K, Laine T, Kuisma S, Nissila J, Hautojärvi P, Dobrzynski L, Baranowski J, Pakula M, Stepniewski K and Porowski S 1997 *Phys. Rev. Lett.* **79** 3030
[13] Brandes G R, Mills A P Jr and Zuckerman D M 1992 *Mater. Sci. Forum* **105-110** 1363
[14] Störmer J, Goodyear A, Anwand W, Brauer G, Coleman P G and Triftäauser W 1996 *J. Phys. Condens. Matter* **8** L89
[15] Jogensen L.V, ven Veen A and Schut H 1996 *Nucl. Phys.* B **119** 487
[16] Suzuki R, Ohdaira T, Uedono A *et al* 1997 *Mater. Sci. Forum* **255-257** 714
[17] Lynn K G and Mckee B T A 1979 *Appl. Phys.* **19** 247
[18] Suzuki R, Ohdaira I, Uedono A *et al* 1997 *Mater. Sci. Forum* **255-257** 114
[19] MacKenzie I K, Eady J A and Ginderlich R R 1970 *Phys. Lett.* A **33** 135
[20] Suzuki R and Ohdaira T 1998 *Jpn. J Appl. Phys.* **37** 4636
[21] van Veen A, Schut H, de Vries R A J, Hakvoort R A and Ijpma M R *Positron Beams for Solids and Surfaces* edited by Schultz P J, Massoumi G R and Simpson P J 1990 *AIP Conference Proceedings* **218** 171
[22] Schultz P J and Lynn K G 1988 *Rev. Mod. Phys.* **60** 701
[23] Puska M, Lanki J P and Nieminen R M 1989 *J. Phys. Condens Matter* **1** 6081
[24] Lundqvist S and March N H 1983 *Theory of the Inhomogeneous Electron Gas* (New York: Plenum)
[25] Andersen O K, Jepsen O and Glotzel D 1985 *Highlights of Condensed Matter Theory* edited by Basni F, Fumi F and Tosi M P (Amsterdam: North-Holland) p59
[26] Skriver H L 1984 *The LMTO Method* (New York: Springer)
[27] Kalinina E V, Kuznetsov N I, Babanin A I, Dmitriev V A and Shchukarev A V 1997 *Diamond and Related Materials* **6** 1528
[28] Jørgensen L V 1998 *PhD Thesis* (Delft University Press, Netherlands)
[29] Alok D, McLarty P K and Baliga B J 1994 *Appl. Phys. Lett.* **64** 2845
[30] Beling C D, Fung S, Li M, Gong M and Panda B K 1999 *Appl. Surf. Sci.* **149** 253